Physics and Chemistry of Minerals (2020) 47:49
https://doi.org/10.1007/s00269-020-01119-1

ORIGINAL PAPER

Saranovskite, $SrCaFe^{2+}_2(Cr_4Ti_2)Ti_{12}O_{38}$, a new crichtonite-group mineral

Nikita V. Chukanov[1,2] · Ramiza K. Rastsvetaeva[3] · Olga N. Kazheva[1] · Oleg K. Ivanov[4] · Igor V. Pekov[2,5] · Atali A. Agakhanov[6] · Konstantin V. Van[7] · Vasiliy D. Shcherbakov[2] · Sergey N. Britvin[8]

Received: 16 August 2020 / Accepted: 9 October 2020 / Published online: 20 October 2020

Abstract

The new crichtonite-group mineral saranovskite, ideally $SrCaFe^{2+}_2(Cr_4Ti_2)Ti_{12}O_{38}$, was discovered in the Glavnoe Saranovskoe deposit, Middle Urals, Russia, and named after the type locality. The associated minerals are chromite, Cr-bearing clinochlore, and calcite. Saranovskite forms black crude equant crystals about 2 mm across. The lustre is submetallic, and the streak is brownish-gray. Cleavage is not observed. The Mohs hardness is 6. Density calculated using the empirical formula is equal to 4.501 g cm^{-3}. The reflectance spectra in visible range are given. The IR spectrum shows the absence of H-, B- and C-bearing groups. The Raman spectrum of saranovskite confirms the absence of H-bearing groups and indicates a rather high degree of ordering of Ti^{4+} and lower-valence cations. The chemical composition of saranovskite is (wt.%; electron microprobe, total iron apportioned between FeO and Fe_2O_3 taking into account charge balance): MgO 2.01, CaO 1.43, MnO 0.21, FeO 8.14, SrO 3.27, BaO 2.18, Al_2O_3 0.53, Sc_2O_3 0.69, Cr_2O_3 10.27, Fe_2O_3 2.19, Y_2O_3 1.56, La_2O_3 0.94, Ce_2O_3 0.91, Pr_2O_3 0.14, Nd_2O_3 0.35, TiO_2 64.25, ZrO_2 0.58, total 99.65. The crystal chemical formula of saranovskite is $(Sr_{0.55}Ba_{0.25}Ln_{0.10}Ca_{0.10})(Ca_{0.36}Y_{0.25}Ln_{0.16}Fe^{2+}_{0.08}Zr_{0.10}Mn_{0.05})$ $(Fe^{2+}_{1.12}Mg_{0.88})(Cr^{3+}_{2.34}Ti_{2.28}Fe^{2+}_{0.91}Fe^{3+}_{0.11}Al_{0.18}Sc^{3+}_{0.18})$ $(Ti_{5.82}Fe^{3+}_{0.18})Ti_{6.0}O_{38}$. The idealized formula is $SrCaFe^{2+}_2(Cr_4Ti_2)Ti_{12}O_{38}$. The crystal structure was determined using single-crystal X-ray diffraction data and refined to $R = 0.0243$. The new mineral is isostructural to other crichtonite-group members. Saranovskite is trigonal, space group $R\bar{3}$, with $a = 10.3553(2)$ Å, $c = 20.7301(4)$ Å, $V = 1925.12(8)$ Å^3 and $Z = 3$. The strongest lines of the powder X-ray diffraction pattern [*d*, Å (*I*, %) (*hkl*)] are: 3.398 (75) (024), 2.881 (100) (– 126), 2.842 (65) (– 234), 2.247 (67) (– 144). 2.137 (76) (– 345), 1.799 (63) (– 348), 1.597 (72) (– 1.4.10, 152), 1.439 (76) (520).

Keywords Saranovskite · New mineral · Crichtonite group · Crystal structure · IR spectroscopy · Raman spectroscopy · Glavnoe Saranovskoe deposit · Middle urals

Oleg K. Ivanov deceased 01 February 2020.

✉ Nikita V. Chukanov
chukanov@icp.ac.ru

[1] Institute of Problems of Chemical Physics, Russian Academy of Sciences, Moscow Region, Chernogolovka 142432, Russia

[2] Faculty of Geology, Moscow State University, Vorobievy Gory, Moscow 119991, Russia

[3] FSRC "Crystallography and Photonics", Russian Academy of Sciences, Leninskii pr. 59, Moscow 119333, Russia

[4] Institute of Geology and Geochemistry, of Urals Branch of Russian Academy of Sciences, Vonsovsky Street 15, Yekaterinburg 620015, Russia

[5] Vernadsky Institute of Geochemistry and Analytical Chemistry, Russian Academy of Sciences, Kosygina Str. 19, 119991 Moscow, Russia

[6] Fersman Mineralogical Museum of the Russian Academy of Sciences, Leninsky Prospekt 8-2, Moscow 119071, Russia

[7] Institute of Experimental Mineralogy, Russian Academy of Sciences, Moscow region, Chernogolovka 142432, Russia

[8] Department of Crystallography, Institute of Earth Sciences, Saint Petersburg State University, Universitetskaya Nab. 7/9, 199034 Saint Petersburg, Russia

Introduction

Minerals belonging to the crichtonite group crystallize in the space group $R\bar{3}$ and have the general crystal chemical formula $^{XII}M0^{VI}M1^{IV}M2_2{}^{VI}M3_6{}^{VI}M4_6{}^{VI}M5_6O_{38}$ in which Roman numerals indicate coordination numbers. The *M*4 and *M*5 sites have octahedral coordination and are predominantly occupied by Ti in all crichtonite-group minerals except paseroite in which these sites may be V^{5+}-dominant (Mills et al. 2012). The cations which were identified at other sites are: *M*0 = Ba, K, Pb, Sr, La, Ce, Na, Ca; *M*1 = Mn^{2+}, Y, U, Fe^{2+}, Zr, Ca, Sc; *M*2 = Fe^{2+}, Mn^{2+}, Mg, Zn; *M*3 = Fe^{3+}, Cr^{3+}, Mn^{3+}, V^{5+}, Al (Mills et al. 2012). The new mineral saranovskite described in this paper is the first chromium member of the crichtonite group which is Sr-dominant at the *M*0 site.

Saranovskite is named after its discovery locality, the famous, historical Saranovskoe chromite deposit (now Glavnoe Saranovskoe). The new mineral and its name were approved by the IMA CNMNC (IMA no. 2020-015). The holotype specimen is deposited in the collections of the Fersman Mineralogical Museum of the Russian Academy of Sciences, Moscow, Russia with the registration number 5558/1.

Experimental methods

Five electron microprobe analyses were carried out using a digital scanning electron microscope Tescan VEGA-II XMU equipped by an Oxford INCA Wave 700 spectrometer (WDS mode, accelerating voltage of 20 kV, electron beam current of 20 nA, beam diameter of 0.3 μm). External standards used for calibration are reported in Table 3. All experimental data including vibrational spectra and X-ray diffraction patterns have been obtained on fragments of the crystal used for the WDS analyses.

To obtain an IR absorption spectrum, saranovskite powder was mixed with anhydrous KBr, pelletized, and analyzed using an ALPHA FTIR spectrometer (Bruker Optics) at a resolution of 4 cm^{-1}. 16 scans were collected. The IR spectrum of an analogous pellet of pure KBr was used as a reference.

Raman spectra were collected in the range of 100–3900 cm^{-1} using a Horiba XploRa confocal Raman spectrometer with the exciting wavelength of 532 nm and 1800 T diffraction grating providing a spectral resolution ~ 1 cm^{-1}. Spectra were collected for 30 s for each spectral window.

Reflectance values for saranovskite have been measured in air using WTiC as a standard by means of a Universal Microspectrophotometer UMSP 50 (Opton-Zeiss, Germany).

Powder X-ray diffraction data were collected with a Rigaku R-AXIS Rapid II single-crystal diffractometer equipped with cylindrical image plate detector using Debye–Scherrer geometry (d = 127.4 mm). Co$K\alpha$ radiation with λ = 1.79021 Å was employed. The data were integrated using the software package osc2tab (Britvin et al. 2017).

Single-crystal X-ray studies were carried out at 293 K with an Xcalibur Eos CCD Oxford Diffraction diffractometer using Mo$K\alpha$ radiation. A total of 32 004 reflections in the θ range of 3.936–51.887° were measured. The crystal structure of saranovskite was solved by direct methods using the AREN program package (Andrianov 1987) and refined by the full-matrix least squares method in an anisotropic approximation for all atoms using SHELXL package (Sheldrick 2015) to R = 0.0243. For most cationic sites, mixed atomic scattering curves were used. Crystal data, data collection information and structure refinement details are given in Table 1.

Results

Occurrence, general appearance and physical properties

Saranovskite was found in the single specimen collected in the Rudnaya underground chromite mine (depth 400 m) operating at the Glavnoe Saranovskoe deposit which belongs to the Saranovskaya group of chromite deposits. The mine is located in the town of Sarany, 5 km to the north of the Laki railway station, Gornozavodskiy district, Perm Krai, Middle Urals, Russia (58° 30′ North, 58° 52′ East). For the description of the deposit, see papers by Ivanov (1990, 1997, 2016).

The new mineral occurs in a hydrothermal calcite vein 3 cm thick which crosscut a rock (chromium ore) mainly composed by Al-rich chromite (80–90 vol.%) cemented by fine-grained Cr-bearing clinochlore. Saranovskite crystals overgrow a crust of purple platy crystals of Cr-bearing clinochlore (*i.e.* clinochlore of second generation which crystallized at the hydrothermal stage on the walls of a crack in the ore). Saranovskite forms crude equant crystals about 2 mm across (Fig. 1). Only three crystals were found.

Saranovskite is black, the lustre is submetallic, and the streak is brownish-gray. Cleavage is not observed. The fracture is conchoidal. Saranovskite is brittle. The VHN hardness determined by micro-indentation at load of 200 g is equal to 850 kg/mm^2 (range 799–890 kg/mm^2, n = 6) The Mohs hardness is 6. Density calculated using the empirical

Table 1 Crystal data, data collection information and structure refinement details for saranovskite

Idealized formula	$SrCaFe^{2+}{}_2(Cr_4Ti_2)Ti_{12}O_{38}$
Space group	$R\bar{3}$ (No. 148)
a (Å)	10.3553(2)
c (Å)	20.7301(4)
V (Å^3)	1925.14(5)
Z	3
D_x (g cm^{-3})	4.513
μ (mm^{-1})	9.255
Data collection	
Diffractometer	Xcalibur Eos CCD Oxford diffraction
Radiation	Mo$K\alpha$
Max. Med. Min. dimensions (mm)	$0.2\times0.25\times0.45$
Temperature (K)	293
Reflections measured	32,004
Independent reflections	4825
Independent reflections with $I>2\sigma(I)$	4418
Parameters refined	97
R_{int}	0.0356
θ range for data collection, °	3.936–51.887
$(2\theta)_{max}$	103.77
Index range	$-22<h<22$; $-22<k<22$; $-45<l<42$
Absorption correction	Multi-scan
Refinement	
Final R indices $[I>2\sigma(I)]$ $R1/wR2$	0.0243/0.0535
R indices (all data) $R1/wR2$	0.0282/0.0548
GoF	1.192
$\Delta\rho_{max}$, $\Delta\rho_{min}$ (e Å^{-3})	2.22, – 1.34

Fig. 1 Crystals of saranovskite. The crystal sizes are 1.5× 2× 2 mm

formula and unit-cell parameters obtained from single-crystal X-ray diffraction data is equal to 4.501 g cm^{-3}.

Reflectance spectroscopy in visible range

Under the microscope, saranovskite is gray, with brown internal reflections. Bireflectance is very weak, **ΔR** = 0.17% (589 nm). Anisotropism is weak. Pleochroism is not observed.

Reflectance values are given in Table 2 (the reference wavelengths required by the Commission on Ore Mineralogy are given in bold type).

Infrared absorption spectroscopy

The IR spectrum of saranovskite (Fig. 2) is rather close to the IR spectra of other crichtonite-group minerals (Chukanov 2014; Chukanov and Chervonnyi 2016). Wavenumbers of absorption bands in the IR spectrum of saranovskite and their assignments are (cm^{-1}, s—strong band, w—weak band, sh—shoulder): 1175w, 1087w (overtones), 726, 625sh, 604s (Ti–O stretching vibrations), 528s, 505sh, 412, 401 (mainly, *M*–O stretching vibrations where *M* = Cr, Fe, Mg, Al, Sc).

The absence of absorption bands above 1200 cm^{-1} indicates the absence of H-, B- and C-bearing groups.

Raman spectroscopy

The Raman spectrum of saranovskite (Fig. 3) confirms the absence of bands of O–H stretching vibrations (in the range of 2500–3900 cm^{-1}). The assignment of the Raman bands is as follows:

- 654 to 800 cm^{-1}–Ti–O stretching vibrations;
- 440 cm^{-1}–$R1^{3+}$–O stretching vibrations (R1 = Cr, Fe, Sc, Al);
- 417 cm^{-1}–$R2^{2+}$–O stretching vibrations (R2 = Mg, Fe);

Table 2 Reflectance values of saranovskite, %

λ (nm)	R_1	R_2	λ (nm)	R_1	R_2
400	19.7	20.2	560	17.5	17.7
420	19.4	19.6	580	17.5	17.7
440	19.1	19.3	589	17.4	17.6
460	18.7	19.9	600	17.3	17.5
470	18.4	19.1	620	17.3	17.5
480	18.5	18.6	640	17.2	17.4
500	18.3	18.4	650	17.2	17.5
520	18.00	18.3	660	17.1	17.3
540	17.6	18.1	680	17.1	17.2
546	17.6	17.9	700	17.1	17.1

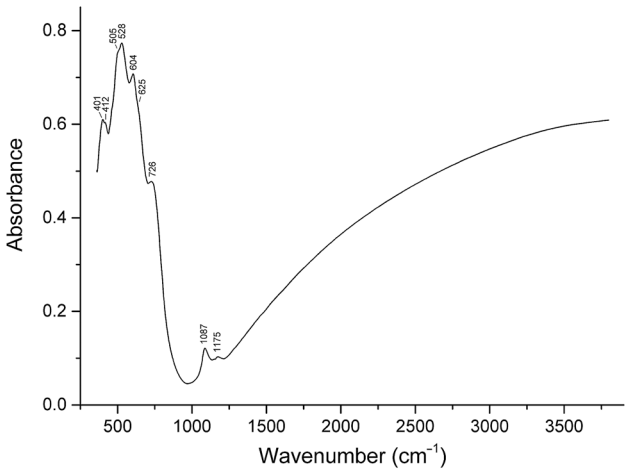

Fig. 2 Powder infrared absorption spectrum of saranovskite

- Below 400 cm^{-1}–lattice modes involving stretching vibrations of lower force-strength cations (Ca, Sr, *REE*) and different kinds of bending vibrations.
- Weak bands in the range of 1200–1600 cm^{-1}—overtones and combination modes.

The assignment of the bands at 654, 735 and 800 cm^{-1} to Ti–O stretching vibrations is based on the fact that Ti^{4+} is the most high force–strength cation occurring in saranovskite. The strongest and the most high-frequency band in this region observed at 800 cm^{-1} may correspond to symmetric stretching vibrations of the Ti–O–Ti bridges with the shortest Ti–O bonds. Analogous strong bands are observed in the Raman spectra of other crichtonite-group minerals: crichtonite (at 809 cm^{-1}: RRUFF database, R060314), dessauite-(Y) and mathiasite (at 812 cm^{-1} for both: Bittarello et al. 2014). However, in the Raman spectra of metamict samples

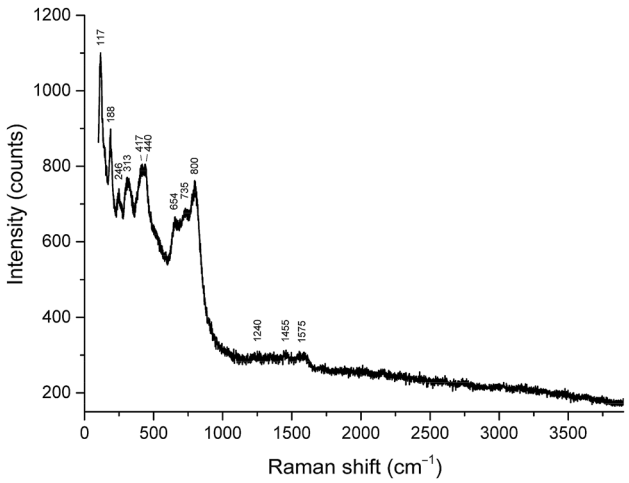

Fig. 3 Raman spectrum of saranovskite

(Frost and Reddy 2011) and synthetic crychtonite-related compounds with disordered structures, synthesized at high temperatures (Konzett et al. 2005), bands in the range of 770–850 cm^{-1} are very weak or are observed as broad shoulders, respectively. Consequently, the presence of the strong band at 800 cm^{-1} in the Raman spectrum of saranovskite indicates a high degree of ordering of Ti^{4+} and other cations having octahedral coordination.

Chemical composition

Analytical data for saranovskite based on five spot analyses of a polished section are given in Table 3. Contents of other elements are below detection limits. In BSE, the mineral is completely uniform. The rim is slightly enriched in Sr and Cr and depleted in Ba as compared to the core, but in all analyses, Sr prevails over Ba in atomic units. H_2O and CO_2 were not measured because no bands corresponding to CO_3^{2-} anions and H-bearing groups are observed in the IR spectrum.

The empirical formula could not be calculated based on 38 O atoms per formula unit (*apfu*) because the Fe^{2+}:Fe^{3+} ratio was not determined experimentally. For this reason, formula coefficients given in Table 3 were calculated based on the sum of 22 metal cations *pfu*, in accordance with structural data (see below). The Fe^{2+}:Fe^{3+} ratio was calculated from the charge-balance requirement, taking into account the fact that the IR spectrum shows the absence of OH groups.

The simplified formula derived based on structural data is $(Sr,Ba)(Ca,Y,Ln)(Fe^{2+},Mg)_2(Cr,Ti)_6Ti_{12}O_{38}$. The idealized end-member formula is $SrCaFe^{2+}{}_2(Cr_4Ti_2)Ti_{12}O_{38}$.

X-ray diffraction data and crystal structure

Powder X-ray diffraction data of saranovskite are given in Table 4. The hexagonal unit-cell parameters refined from the powder data are: $a = 10.372(1)$, $c = 20.808(4)$ Å; $V = 1938.8(8)$ $Å^3$. The systematic absences of reflections are in agreement with the space group $R\bar{3}$ determined from the single-crystal X-ray diffraction data.

The crystal structure of saranovskite (Fig. 4, Tables 5, 6 and 7) is consistent with that reported for all other members of the crichtonite group. It is based on a close-packed framework with a nine-layer stacking sequence $[chhchhchh]_\infty$. Large cations, namely Sr, Ba and subordinate Ca and *LREE*, occur at the 12-coordinated *M*0 site. The *M*1 octahedron is occupied by the largest octahedral cations, Ca, REE^{3+}, and minor Zr, Mn^{2+} and Fe^{2+}; Fe^{2+} and subordinate Mg occupy the *M*2 tetrahedron. The smallest, distorted *M*4- and *M*5-centered octahedra are mainly occupied by Ti atoms. The bond valence sums (BVS) at the *M*4 and *M*5 sites are equal to 4.04 and 3.99, respectively (Table 7). The *M*3 site with a more regular octahedral coordination and BVS of

Table 3 Chemical composition of saranovskite

Constituent	Content, wt.%	Range	Standard deviation	Formula coefficient	Standard
MgO	2.01	1.74–2.30	0.19	0.87	Diopside
CaO	1.43	1.20–1.60	0.13	0.45	Wollastonite
MnO	0.21	0–0.37	0.12	0.05	Mn
FeO*	8.14	9.64–10.66**	0.35**	1.98	Fe
Fe_2O_3*	2.19			0.48	
SrO	3.27	2.98–3.70	0.23	0.55	SrF_2
BaO	2.18	1.59–2.68	0.41	0.25	BaF_2
Al_2O_3	0.53	0.38–0.76	0.13	0.18	Albite
Sc_2O_3	0.69	0.57–0.86	0.10	0.18	Sc
Cr_2O_3	10.27	9.42–11.41	0.76	2.36	Cr
Y_2O_3	1.56	1.29–1.80	0.19	0.24	YPO_4
La_2O_3	0.94	0.77–1.34	0.20	0.10	$LaPO_4$
Ce_2O_3	0.91	0.73–1.17	0.17	0.10	$CePO_4$
Pr_2O_3	0.14	0–0.27	0.08	0.02	$PrPO_4$
Nd_2O_3	0.35	0.22–0.48	0.09	0.04	$NdPO_4$
TiO_2	64.25	63.13–64.94	0.62	14.07	Ti
ZrO_2	0.58	0.45–0.71	0.10	0.06	Zr
Total	99.65				

*Total iron (corresponding to 10.12 wt% FeO) was apportioned between FeO and Fe_2O_3 taking into account charge balance

**For total iron calculated as FeO

Table 4 Powder X-ray diffraction data (d in Å) of saranovskite

I_{obs}	d_{obs}	I_{calc}*	d_{calc}**	$h\ k\ l$	I_{obs}	d_{obs}	I_{calc}*	d_{calc}**	$h\ k\ l$
8	8.25	6	8.231	101	12	1.695	7	1.695	054
7	4.503	5	4.487	104			2	1.690	327
10	4.389	7	4.383	021			3	1.689	241
17	4.140	10	4.144	113	14	1.649	11	1.646	505
		8	4.115	202	14	1.613	1	1.611	− 258
20	3.773	19	3.763	015			11	1.611	− 264
75	3.398	75	3.391	024	72	1.597	78	1.592	− 1.4.10
6	3.349	3	3.345	211			2	1.592	152
9	3.227	6	3.222	122	15	1.572	2	1.570	1.0.13
48	3.052	50	3.044	205			12	1.569	425
34	2.993	32	2.989	300	17	1.546	13	1.544	− 366
100	2.881	100	2.874	− 126	15	1.543	8	1.538	− 564
65	2.842	64	2.837	− 234	5	1.526	3	1.522	4.0.10
32	2.748	36	2.744	303	31	1.506	29	1.502	− 3.4.11
30	2.630	35	2.624	− 135			4	1.501	155
7	2.591	8	2.589	220	6	1.496	1	1.495	600
45	2.474	47	2.470	131			4	1.491	− 459
38	2.425	18	2.424	− 243	4	1.474	2	1.471	− 267
		22	2.419	312	9	1.463	2	1.461	603
2	2.309	2	2.303	009			2	1.460	− 3.5.10
67	2.247	60	2.242	− 144			3	1.460	342
76	2.137	68	2.133	− 345	8	1.449	6	1.443	− 2.3.13
8	2.111	7	2.104	119	76	1.439	92	1.436	520
4	2.064	3	2.059	− 138	11	1.421	1	1.418	− 468
6	2.024	3	2.020	1.0.10			8	1.418	434
		2	2.018	232	12	1.410	6	1.406	2.0.14
3	1.976	2	1.972	045			7	1.406	− 573
9	1.960	8	1.957	410	8	1.392	1	1.390	− 2.5.11
22	1.913	15	1.912	324			7	1.389	− 375
		10	1.905	137	15	1.375	15	1.372	606
10	1.887	5	1.883	− 453	7	1.362	1	1.365	161
		3	1.882	0.2.10			7	1.357	− 1.3.14
16	1.847	14	1.843	235	9	1.346	10	1.342	− 1.4.13
63	1.799	59	1.794	− 348	6	1.340	6	1.335	− 1.2.15
12	1.774	11	1.768	2.1.10	3	1.323	1	1.322	− 174
6	1.733	5	1.728	0.0.12			2	1.320	− 477
34	1.706	30	1.703	146					

*For the calculated pattern, only reflections with intensities ≥ 1 are given

**For the unit-cell parameters calculated from single-crystal data

3.29 concentrates trivalent cations with ionic radii in the range of 0.62–0.73 Å (Shannon 1976), as well as remaining Ti^{4+} and Fe^{2+} cations.

The crystal chemical formula of saranovskite can be written as follows ($Z=3$): $^{M0}(Sr_{0.55}Ba_{0.25}Ln_{0.10}Ca_{0.10})^{XII\,M1}(Ca_{0.36}Y_{0.25}Ln_{0.16}Fe^{2+}_{0.08}Zr_{0.10}Mn_{0.05})^{VI\,M2}(Fe^{2+}_{1.12}Mg_{0.88})^{IV\,M3}(Cr^{3+}_{2.34}Ti_{2.28}Fe^{2+}_{0.91}Fe^{3+}_{0.11}Al_{0.18}Sc^{3+}_{0.18})^{VI\,M4}(Ti_{5.82}Fe^{3+}_{0.18})^{VI}{}_{M5}Ti_{6.0}{}^{VI}O_{38}$ where Roman numerals indicate coordination numbers of cations and the Fe^{2+}:Fe^{3+} ratio was calculated based on the charge-balance requirement.

The mean charges of cationic sites are in a good agreement with the BVS values (Table 7). In particular, the $M3$ site is dominated by trivalent cations among which Cr is the most abundant: $Fe^{2+}_{0.15}(Cr^{3+}_{0.39}Al^{3+}_{0.03}Sc^{3+}_{0.03}Fe^{3+}_{0.02})_{\Sigma 0.47}Ti^{4+}_{0.38}$. Thus, according to the dominant valency rule, Ca and Cr are the species-defining components, and the idealized formula of saranovskite is $SrCaFe^{2+}{}_2(Cr_4Ti_2)Ti_{12}O_{38}$.

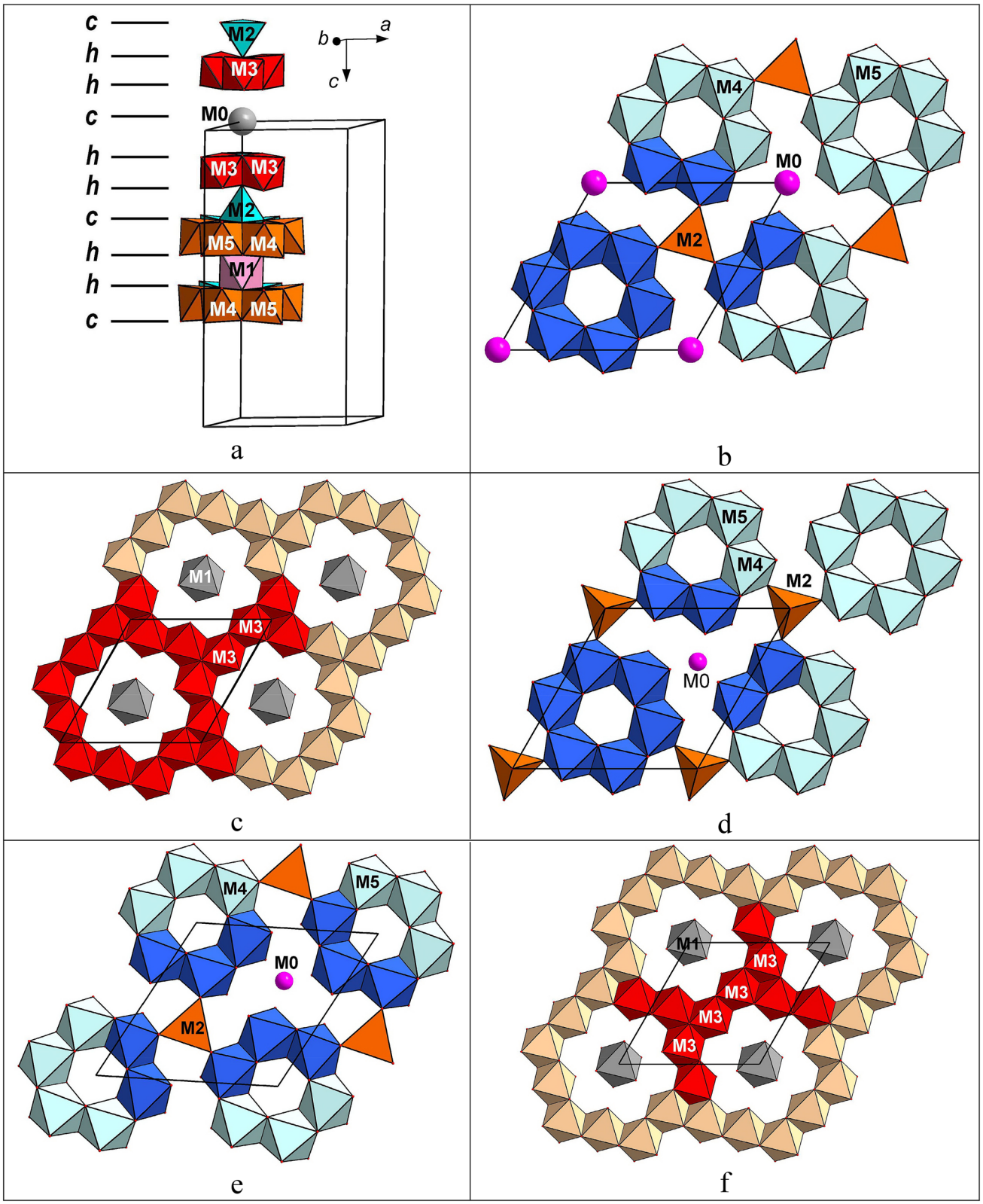

Fig. 4 Mutual arrangement of the polyhedral *c* and *h* layers in the crystal structure of saranovskite (**a**) and separate layers viewed down the *c* axis: the levels $c \approx 0.06$ (**b**), $c \approx 0.16$ (**c**), $c \approx 0.26$ (**d**), $c \approx 0.39$ (**e**), and $c \approx 0.49$ (**f**). The unit cell is outlined

Table 5 Site coordinates and multiplicities (Q), equivalent displacement parameters of atoms (U_{eq}, Å^2) and site compositions for saranovskite

Site*	x	y	z	Q	U_{eq}	Composition
*M*0	0	0	0	3	0.00930 (3)	$Sr_{0.55}Ba_{0.25}Ce_{0.10}Ca_{0.10}$
*M*1	0.333333	0.666667	0.166667	3	0.00562 (3)	$Ca_{0.36}Y_{0.25}Fe^{2+}_{0.08}Zr_{0.1}Ce_{0.16}Mn_{0.05}$
*M*2	0.666667	0.333333	0.02320 (2)	6	0.00580 (4)	$Fe_{0.56}Mg_{0.44}$
*M*3	0.18240 (2)	0.04253 (2)	0.16458 (2)	18	0.00487 (2)	$Cr_{0.39}Ti_{0.38}(Fe^{2+},Fe^{3+})_{0.17}Al_{0.03}Sc_{0.03}$
*M*4	0.57764 (2)	0.59201 (2)	0.06586 (2)	18	0.00527 (2)	$Ti_{0.97}(Fe^{2+},Fe^{3+})_{0.03}$
*M*5	0.25197 (2)	0.33917 (2)	0.05941 (2)	18	0.00575 (2)	$Ti_{1.0}$
O1	0.59248 (7)	0.02784 (7)	0.10758 (3)	18	0.00546 (8)	$O_{1.0}$
O2	0.06383 (7)	0.29762 (7)	0.00735 (3)	18	0.00583 (8)	$O_{1.0}$
O3	0.36734 (7)	0.10749 (7)	0.11740 (3)	18	0.00593 (9)	$O_{1.0}$
O4	0.12775 (7)	0.16980 (7)	0.10915 (3)	18	0.00631 (9)	$O_{1.0}$
O5	0.19985 (7)	0.47428 (7)	0.10316 (3)	18	0.00722 (9)	$O_{1.0}$
O6	0.61383 (7)	0.48347 (7)	– 0.00406 (3)	18	0.00488 (8)	$O_{1.0}$
O7	0.666667	0.333333	0.12059 (5)	6	0.0051 (1)	$O_{1.0}$

*Designated afterArmbruster and Kunz (1990)

Table 6 Selected cation-oxygen distances (Å) in saranovskite

*M*0	O4	2.7632 (6)×6	*M*4	O3	1.8553 (6)
	O2	2.8144 (6)×6		O5	1.8824 (6)
		<2.789>		O1	1.9375 (6)
*M*1	O5	2.2043 (7)×6		O6	1.9813 (6)
		<2.204>		O2	2.0159 (6)
*M*2	O6	1.9715 (6)×3		O6	2.1526 (6)
	O7	2.019 (1)			<1.971>
		<1.981>	*M*5	O4	1.8809 (6)
*M*3	O3	1.9463 (6)		O1	1.9391 (6)
	O3	1.9760 (6)		O5	1.9561 (7)
	O1	1.9844 (6)			
	O7	1.9818 (5)		O2	1.9611 (6)
	O4	2.0305 (6)		O6	2.0171 (6)
	O4	1.9947 (6)		O2	2.0754 (6)
		<1.985>			<1.972>

Discussion

In all crichtonite-group minerals, the *M*4 and *M*5 sites are Ti-dominated. Thus, the crystal-chemical diversity of these minerals is mainly determined by the components occurring at the *M*0–*M*3 sites. The dominant components at the species-defining key sites of different members of the crichtonite group are given in Table 8.

Saranovskite is the Ca-dominant (at the *M*1 site) and Cr^{3+}-dominant (at the *M*4 site) analogue of crichtonite, ideally $SrMn^{2+}Fe^{2+}_2(Fe^{3+}_4Ti_2)Ti_{12}O_{38}$ (Grey et al. 1976). Another crichtonite-group mineral chemically related to saranovskite is dessauite-(Y), $(Sr,Pb)(Y,U)(Ti,Fe^{3+})_{20}O_{38}$ (Orlandi et al. 1997). Comparative data for saranovskite and some related (Sr-dominant) crichtonite-group minerals are given in Table 9. It is to be noted that saranovskite is not the first member of the crichtonite group with species-defining Cr. Other two Cr-dominant (at the *M*3 site) crichtonite-group minerals are lindsleyite (Zhang et al. 1988) and mathiasite (Gatehouse et al. 1983) (see Table 8).

Saranovskite is a hydrothermal mineral probably formed as a result of the interaction of chromite ore (chromitite)

Table 7 Bond-valence calculations for saranovskite

	O1	O2	O3	O4	O5	O6	O7	Σ
M0		$0.17^{\rightarrow x6}$		$0.19^{\rightarrow x6}$				2.16
M1					$0.54^{\rightarrow x6}$			3.24
M2						$0.50^{\rightarrow x3}$	0.44	1.94
M3	0.55		0.61 + 0.56	0.49 + 0.53			$0.55^{\downarrow x3}$	3.29
M4	0.71	0.58	0.89		0.83	0.63 + 0.40		4.04
M5	0.72	0.67 + 0.50		0.84	0.68	0.58		3.99
Σ	1.98	1.92	2.06	2.05	2.05	2.11	2.09	

Bond-valence parameters were taken from Brese and O`Keeffe (1991)

Table 8 Dominant (species-defining) components at the key sites in crichtonite-group minerals

Mineral	Key sites				Reference
	*M*0	*M*1	*M*2	*M*3	
Landauite	Na	Mn^{2+}	Zn	Ti (?)	Grey and Gatehouse (1978)
Loveringite	Ca	Zr	Mg	Fe^{3+}	Gatehouse et al. (1978)
Lindsleyite	Ba	Zr	Mg	Cr^{3+}	Zhang et al. (1988)
Mathiasite	K	Zr	Mg	Cr^{3+}	Gatehouse et al. (1983)
Davidite-(La)	La	Y	Fe^{2+}	Fe^{3+}	Gatehouse et al. (1979)
Davidite-(Ce)	Ce	Y	Fe^{2+}	Fe^{3+}	Gatehouse et al. (1979)
Crichtonite	Sr	Mn^{2+}	Fe^{2+}	Fe^{3+}	Grey et al. (1976)
Dessauite-(Y)	Sr	Y	Fe^{2+}	Fe^{3+}	Orlandi et al. (1997)
Senaite	Pb	Mn^{2+}	Fe^{2+}	Fe^{3+}	Grey and Lloyd (1976)
Gramaccioliite-(Y)	Pb	Y	Fe^{2+}	Fe^{3+}	Orlandi et al. (2004)
Cleusonite	Pb	U^{4+}	Fe^{2+}	Fe^{2+} (?)	Wülser et al. (2005)
Paseroite	Pb	Mn^{2+}	Fe^{3+}	V^{5+} (?)	Mills et al. (2012)
Mapiquiroite	Sr	U^{4+}	Fe^{2+}	Fe^{3+}	Biagioni et al. (2014)
Almeidaite	Pb	Mn^{2+}	Zn	Fe^{3+}	Rastsvetaeva et al. (2014), Menezes Filho et al. (2015)
Saranovskite	Sr	Ca	Fe^{2+}	Cr^{3+}	This work

Table 9 Comparative data for Sr-dominant crichtonite-group minerals

Mineral	Saranovskite	Crichtonite	Dessauite-(Y)	Mapiquiroite
Simplified formula	$SrCaFe^{2+}_2(Cr_4Ti_2)Ti_{12}O_{38}$	$SrCaFe^{2+}_2(Fe^{3+}_4Ti_2)Ti_{12}O_{38}$	$SrYFe^{2+}_2(Fe^{3+}_5Ti)Ti_{12}O_{38}$	$SrU^{4+}Fe_2{}^{2+}Fe^{3+}_6Ti_{12}O_{38}$
Crystal system	Trigonal			
Space group	$R\bar{3}$			
a, Å	10.3553	10.373	10.373	10.3719
c, Å	20.7301	20.745	20.746	20.875
V, Å^3	1925.14	1933.2	1933.5	1944.8
Z	3	3	3	3
Strongest reflections of the powder X-ray diffraction pattern: *d*, Å (*I*, %)	3.398 (75) 2.881 (100) 2.842 (65) 2.247 (67) 2.137 (76) 1.799 (63) 1.597 (72) 1.439 (76)	3.395 (71) 3.048 (63) 2.877 (100) 2.841 (67) 2.474 (51) 2.136 (54) 1.594 (62) 1.439 (59)	3.412 (m) 2.902 (m) 2.846 (mw) 2.499 (mw) 1.916 (mw) 1.805 (mw) 1.603 (m) 1.441 (m)	6.81 (76) 5.18 (100) 4.51 (44) 4.125 (29) 3.404 (41) 2.994 (35) 2.889 (29)
Density, g cm^{-3}	4.501 (calc.)	4.54 (calc.)	4.68 (calc.)	4.483 (calc.)
References	This work	Hey et al. (1969), Grey et al. (1976)	Orlandi et al. (1997)	Biagioni et al. (2014)

with fluid derived by a diabase intrusion (Ivanov 1990, 2016). During the formation of veins which crosscut chromitite bodies at the Glavnoe Saranovskoe deposit and the neighboring Yuzhno-Saranovskoe (Biserskoe) deposit, chromium activity in hydrothermal solutions was very high which resulted in the crystallization of a unique, in both diversity and gross amount, assemblage of silicates and oxides/hydroxides containing Cr^{3+} as a species-defining component or important admixture (several wt.%). We did not find in literature data on another locality with a similar species diversity of hydrothermal Cr-rich minerals.

The Cr-bearing silicates found in hydrothermal veins of Glavnoe Saranovskoe and Yuzhno-Saranovskoe chromite deposits are grossular–***uvarovite*** series garnets, pumpellyite-group members forming the pumpellyite-(Mg)–***shuiskite-(Mg)–shuiskite-(Cr)*** series, celadonite–***chromceladonite*** series micas and Cr-rich varieties of titanite, zoisite, muscovite, clinochlore, and amesite. Hydrothermal chromium-rich

oxides and hydroxides are represented here by two polymorphs of CrOOH, namely ***grimaldiite*** and ***guyanaite***, ***redledgeite***, ***saranovskite***, ***stichtite*** and Cr-rich varieties of rutile, diaspore, kassite, and pyroaurite (minerals with species-defining Cr^{3+} are marked with bold italic) (Ivanov 2016; Lykova et al. 2018, 2020; Sustavov et al. 2019; this work). Saranovskite is the first Sr- and *REE*-enriched mineral in these hydrothermal veins. For this mineral, chromite was the source of Cr, diabase was the most probable source of Ti, while other components including Ca, Sr, Ba and *REE* could be extracted by the hydrothermal fluid from diabase or/and carbonate-bearing host rocks.

Cr-rich crichtonite-group minerals are quite common in ultramafic rocks (chromitites, gabbronorites, pyroxenites, kimberlites etc.) (Gatehouse et al. 1983; Zhang et al. 1988; Chukanov et al. 2019). In particular, Cr-rich loveringite was described in the Western Laouni layered complex, Southern Hoggar, Algeria (with 7.0% Cr_2O_3, *i.e.* 1.54 *apfu* Cr: Lorand et al. 1987), in Last-Yavr mafic–ultramafic intrusion, Kola Peninsula (with 7.11% Cr_2O_3, *i.e.* 1.67 *apfu* Cr: Barkov et al. 1996) and in the Koitelainen layered intrusion, Northern Finland (with 7.6% Cr_2O_3, *i.e.* 1.94 *apfu* Cr: Tarkian and Mutanen 1987). Mathiasite chromium analogue from the Obnazhennaya kimberlite pipe contains 12.38 wt.% Cr_2O_3 which corresponds to 2.60 *apfu* Cr (Chukanov et al. 2019). However, there are no data on the finds of crichtonite-group minerals in primary chromite ores of the Saranovskoe deposit.

Acknowledgements The authors are grateful to Radek Škoda and an anonymous reviewer for valuable comments. This work was performed in accordance with the state task, state registration no. AAA-A19-119092390076-7 (mineralogical study, single crystal X-ray analysis, and IR spectroscopy) and was partly supported by Lomonosov Moscow State University Program of Development (Raman spectroscopy). The authors thank the SPbSU X-Ray Diffraction Resource Center and Center for Molecule Composition Studies of INEOS RAS for instrumental support.

References

Andrianov VI (1987) AREN-85 system of crystallographical programs RENTGEN for EVM NORD, SM-4 and EC. Crystallogr Rep 32(1):228–232

Armbruster T, Kunz M (1990) Cation arrangement in an unusual uranium-rich senaite crystal structure study at 130 K. Eur J Mineral 2:163–170

Barkov AY, Savchenko YE, Men'shikov YP, Barkova LP (1996) Loveringite from the Last-Yavr mafic-ultramafic intrusion, Kola Peninsula; a second occurrence in Russia. Norsk Geol Tiddsskrift 76:115–120

Biagioni C, Orlandi P, Pasero M, Nestola F, Bindi L (2014) Mapiquiroite, (Sr, Pb)(U, Y)Fe_2(Ti, Fe^{3+})$_{18}O_{38}$, a new member of the crichtonite group from the Apuan Alps, Tuscany, Italy. Eur J Mineral 26:427–437

Bittarello E, Ciriotti ME, Costa E, Gallo LM (2014) "Mohsite" of Colomba: identification as dessauite-(Y). Intern J Mineral. https://doi.org/10.1155/2014/287069

BreseO`Keeffe NEM (1991) Bond-valence parameters for solids. Acta Cryst B47:192–197

Britvin SN, Dolivo-Dobrovolsky DV, Krzhizhanovskaya MG (2017) Software for processing the X-ray powder diffraction data obtained from the curved image plate detector of Rigaku RAXIS Rapid II diffractometer. Zapiski RMO 146(3):104–107

Chukanov NV (2014) Infrared spectra of mineral species: extended library. Springer-Verlag GmbH, Dordrecht–Heidelberg–New York–London, pp. 1716

Chukanov NV, Chervonnyi AD (2016) Infrared spectroscopy of minerals and related compounds. Springer: Cham–Heidelberg–Dordrecht–New York–London, pp. 1109

Chukanov NV, Vorobei SS, Ermolaeva VN, Varlamov DA, Plechov PY, Jančev S, Bovkun AV (2019) New data on chemical composition and vibrational spectra of magnetoplumbite-group minerals. Geol Ore Depos 61:637–646

Frost RL, Reddy BJ (2011) The effect of metamictization on the Raman spectroscopy of the uranyl titanate mineral davidite (La, Ce)(Y, U, Fe^{2+})(Ti, Fe^{3+})$_{20}$(O, OH)$_{38}$. Radiat Eff Defects Solids 166(2):131–136

Gatehouse BM, Grey IE, Campbell IH, Kelly PR (1978) The crystal structure of loveringite – a new member of the crichtonite group. Am Mineral 63:28–36

Gatehouse BM, Grey IE, Kelly PR (1979) The crystal structure of davidite. Am Mineral 64:1010–1017

Gatehouse BM, Grey IE, Smyth JR (1983) Structure refinement of mathiasite, $(K_{0.62}Na_{0.14}Ba_{0.14}Sr_{0.10})_{\Sigma 1.0}[Ti_{12.90}Cr_{3.10}Mg_{1.53}Fe_{2.15}Zr_{0.67}Ca_{0.29}(V, Nb, A_l)_{0.3}]_{\Sigma 21.0}O_{38}$. Acta Cryst C39:421–422

Grey IE, Gatehouse BM (1978) The crystal structure of landauite, $NaMnZn_2(Ti, Fe)_6Ti_{12}O_{38}$. Can Mineral 16:63–68

Grey IE, Lloyd DJ (1976) Crystal structure of senaite. Acta Cryst B32:1509–1513

Grey IE, Lloyd DJ, White JS (1976) The structure of crichtonite and its relationship to senaite. Am Mineral 61:1203–1212

Hey MH, Embrey PG, Fejér EE (1969) Crichtonite, a distinct species. Mineral Mag 37:349–356

Ivanov OK (1990) Layered chromite-bearing ultramafic formations of urals. Moscow: Nedra, pp. 243. (in Russian)

Ivanov OK (1997) Mineral associations of the Saranovskoe chromite deposit. Ekaterinburg: Institute of geology and geochemistry, pp. 123. (in Russian)

Ivanov OK (2016) Mineralogy of the Saranovskoe chromite deposit (Middle Urals). Mineral Alm 21(2):120

Konzett J, Yang H, Frost DJ (2005) Phase relations and stability of magnetoplumbite-and crichtonite-series phases under upper-mantle PT conditions: an experimental study to 15 GPa with implications for LILE metasomatism in the lithospheric mantle. J Petrol 46(4):749–781

Lorand J-P, Cottin J-Y, Parodi GC (1987) Occurrence and petrological significance of loveringite in the Western Laouni layered complex, Southern Hoggar, Algeria. Can Mineral 25:683–693

Lykova IS, Varlamov DA, Chukanov NV, Pekov IV, Zubkova NV (2018) Crystal chemistry of shuiskite and chromian pumpellyite-(Mg). Eur J Mineral 30:1133–1139

Lykova I, Varlamov DA, Chukanov NV, Pekov IV, Belakovskiy DI, Ivanov OK, Zubkova NV, Britvin SN (2020) Chromium members of the pumpellyite group: shuiskite-(Cr), $Ca_2CrCr_2[SiO_4][Si_2O_6(OH)](OH)_2O$, a new mineral, and shuiskite-(Mg), a new species name for shuiskite. Minerals 10:390

Menezes Filho LAD, Chukanov NV, Rastsvetaeva RK, Aksenov SM, Pekov IV, Chaves MLSC, Scholz R, Atencio D, Brandão PRG, Romano A, de Oliveira LCA, Ardisson JD, Krambrock K, Moreira

RL, Guimarães FS, Persiano AC, Richards RP (2015) Almeidaite, $PbZn_2(Mn, Y)(Ti, Fe^{3+})_{18}O_{37}(OH, O)$, a new crichtonite-group mineral, from Novo Horizonte, Bahia, Brazil. Mineral Mag 79:269–283

Mills SJ, Bindi L, Cadoni M, Kampf AR, Ciriotti ME, Ferraris G (2012) Paseroite, $PbMn^{2+}(Mn^{2+}, Fe^{2+})_2(V^{5+}, Ti, Fe^{3+})_{18}{}^{O}{}_{38}$, a new member of the crichtonite group. Eur J Mineral 24:1061–1067

Orlandi P, Pasero M, Duchi G, Olmi F (1997) Dessauite, $(Sr, Pb)(Y, U)(Ti, Fe^{3+})_{20}O_{38}$, a new mineral of the crichtonite group from Buca della Vena mine, Tuscany, Italy. Am Mineral 82:807–811

Orlandi P, Pasero M, Rotiroti N, Olmi F, Demartin F, Moëlo Y (2004) Gramaccioliite-(Y), a new mineral of the crichtonite group from Stura Valley, Piedmont, Italy. Eur J Mineral 16:171–175

Rastsvetaeva RK, Aksenov SM, Chukanov NV, Menezes LAD (2014) The crystal structure of almeidaite, a new mineral of the crichtonite group. Dokl Chem 455:53–57

Rigaku Oxford Diffraction, CrysAlisPro Software System, Version 1.171.39.46 Rigaku Oxford Diffraction: Oxford, UK, 2018

Shannon R (1976) Revised effective ionic radii and systematic studies of interatomic distances in halides and chalcogenides. Acta Cryst A32:751–767

Sheldrick GM (2015) Crystal structure refinement with SHELXL. Acta Cryst C71:3–8

Sustavov SG, Khanin DA, Shagalov ES (2019) Chromceladonite from the Southern Sarany chromite deposit (Northern Urals). Geol Ore Depos 61(7):680–688

Tarkian M, Mutanen T (1987) Loveringite from the Koitelainen Layered Intrusion, Northern Finland. Mineral Petrol 37:37–50

Wülser PA, Meisser N, Brugger J, Schenk K, Ansermet S, Bonin M, Bussy F (2005) Cleusonite, $(Pb, Sr)(U^{4+}, U^{6+})(Fe^{2+}, Zn)_2(Ti, Fe^{2+}, Fe^{3+})_{18}(O, OH)_{38}$, a new mineral species of the crichtonite group from the western Swiss Alps. Eur J Mineral 17:933–942

Zhang J, Ma J, Li L (1988) The crystal structure and crystal chemistry of lindsleyite and mathiasite. Geol Rev 34:132–144